Dynamics of Nanoscale Precursor Film near a Moving Contact Line of Spreading Drops

A. Hoang and H. P. Kavehpour

Complex Fluids and Interfacial Physics Laboratory, Department of Mechanical and Aerospace Engineering, UCLA, Los Angeles, California 90095, USA

(Received 19 January 2011; revised manuscript received 3 May 2011; published 20 June 2011)

The spreading of liquids on solids is a commonplace phenomenon, discernible in various instances of everyday life. Despite the apparent simplicity of spreading, the underlying mechanisms are still not fully understood on a microscopic level, particularly at the moving edge between liquid and solid known as the contact line region. Here we show the time-dependent evolution of nanoscale films on a clean solid surface near the moving contact line. Our work contributes to the body of experimental evidence required to assemble a comprehensive understanding of microstructures at the vicinity of the contact line, bridging the gap between computational methods and theory. Moreover, this research will provide insight into the fundamental behavior of fluid spreading and other surface phenomena.

DOI: 10.1103/PhysRevLett.106.254501 PACS numbers: 47.55.D−, 47.55.nd, 47.55.np, 68.08.Bc

A well-known problem exists for the theory behind spreading fluids on solid surfaces concerning the no-slip boundary condition applied at the interface [1–3]. Far from the contact line, this boundary condition is valid. However, in the immediate vicinity of the contact line, the velocity field becomes multivalued since the free surface condition meets the no-slip condition in this region and the viscous force becomes unbounded. The resulting singularity is problematic because it effectively eliminates a condition necessary to solve the boundary-value problem. Thus, there remains an unresolved discrepancy between theory of fluid spreading and the physical phenomena. Often this problem is avoided by making *ad hoc* assumptions such as introducing a nonzero slip velocity at the moving contact line.

In the spreading of completely wetting fluids, a microscopic film known as the precursor layer may exist at the front of the moving contact line and prewets the solid surface. This layer is significant because its thickness does not go to zero at the contact line. Therefore, the precursor film allows for the velocity field to become single valued and the viscous force to become finite. Cases in which a precursor film forms provide an opportunity to solve for the macroscopic wetting dynamics without resorting to *ad hoc* boundary conditions at the moving contact line.

Precursor films develop when the thickness of the drop approaches submicron dimensions. A representative schematic is presented in Fig. 1, depicting the vicinity of the contact line region where long-range intermolecular forces between the solid and liquid significantly contribute to the formation of the precursor film [4]. Flow within the precursor film is considered one dimensional and can be described by a lubrication analysis. Furthermore, the spreading of the film is decoupled from the spreading of the bulk [4]. The macroscopic spreading follows Tanner's law, also known as the Hoffman-Voinov-Tanner relationship [1,5–8], $\theta_a \propto \mathrm{Ca}^{1/3}$. Here θ_a is the apparent dynamic contact angle and $\mathrm{Ca} = \eta U/\sigma$ is the capillary number, where η is the viscosity, σ is the surface tension, and U is the velocity of the spreading drop.

Spreading of the precursor film, on the other hand, is dominated by van der Waals forces and can be characterized into two main types: adiabatic and diffusive [8]. The adiabatic film forms in earlier stages and moves with a constant velocity with respect to the solid surface [8,9]. The diffusive film develops at later times and results from the balance between van der Waals interactions and viscosity [4,10]. Here we focus on the diffusive precursor film, for which we are able to capture the dynamic evolution using our experimental technique. For van der Waals fluids, we expect the length of the diffusive precursor film to be proportional to the square root of time [4], in the following form:

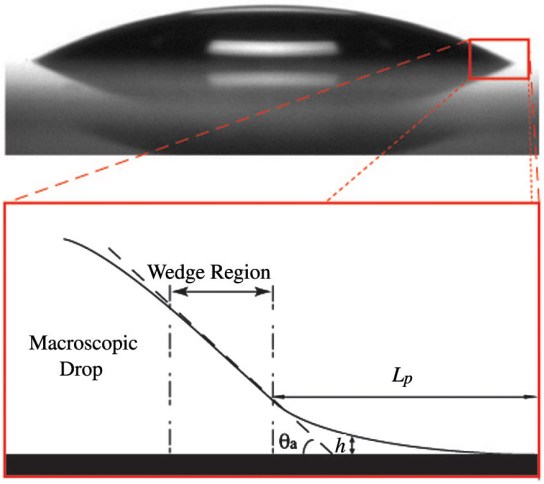

FIG. 1 (color online). Schematic of macroscopic and microscopic features in the vicinity of the advancing contact line for a completely wetting van der Waals fluid spreading on a solid.

$$L_p = \sqrt{\frac{A}{3\pi\eta h_c}} t^{1/2}, \quad (1)$$

where L_p is the length of the precursor film, A is the effective Hamaker constant, η is viscosity, h_c is the cutoff thickness, and t is time. The free surface profile at time t is a function of distance x from the apparent contact line as follows [4]:

$$h(x, t) = \frac{A}{6\pi\eta} t \frac{1}{x^2}. \quad (2)$$

Although the structure of the precursor film has been studied theoretically, previous experimental investigations have been unable to capture the complete scope of the feature. Hardy first reported the existence of the precursor film by observing reduced static friction near spreading drops [11]. Experimental work measuring the film used interferometry [9], ellipsometry [12,13], and polarized reflected microscopy [14,15]. However, even recent measurement techniques [16,17] lacked the adequate range and resolution to fully explore the characteristics of this dynamic phenomenon. Overall, the available experimental data show the existence of the precursor film for an instant of time but do not capture the characteristics of the film as it evolves over time.

To overcome these challenges, we use epifluorescence inverted microscopy to investigate this phenomenon. This technique allows the noninvasive and dynamic measurement of film thickness. The range, resolution, and high signal-to-noise ratio are ideal for the purposes of investigating microstructures in the vicinity of the moving contact line. Although fluorescence microscopy is commonly used in researching life science applications such as cellular dynamics, it has never before been used to study contact line dynamics.

In our experiment, a glass slide (VWR microcover glass, No. 1) is rinsed successively in acetone, methanol, and distilled water and then undergoes plasma cleaning for 30 min, which removes impurities and contaminants using energetic plasma [18]. The Harrick PDC-32G plasma cleaner was used at a high power setting, processing room air. A drop (~ 1 μL) of 10 000 cSt silicone oil (polydimethylsiloxane from Gelest, Inc.), in which a photochromic dye (spironaphthoxazine available from Sigma-Aldrich, Inc.) is fully dissolved, is deposited onto the slide. Note that for a small drop, gravitational effects are negligible and a spherical cap forms in this viscous-capillary regime [19]. The sample is then illuminated from the underside and the signal is collected through the 60× objective lens (NA 1.45) of a Nikon Eclipse TE-2000S microscope with an inverted configuration. With a 150 μm field of view, the lateral resolution is approximately 0.2 μm, which is significantly higher than that offered by other methods such as ellipsometry. The temporal resolution is largely determined by the exposure time and lies around 200 ms for our case, which is much smaller than the time of spreading.

The collected intensity of the dye emission can be related proportionally to the thickness of the thin film according to the Beer-Lambert law, which is valid for thicknesses less than a millimeter [20]. To ensure consistency of the dye's excitation and emission, the drop is saturated with excitation light for approximately 2 h before meaningful data are collected. For this reason, to which we have previously alluded, only the diffusive precursor film is captured. Unlike typical fluorescence dyes, this photochromic dye exhibits a reversible color change and is highly photostable without photodegradation for long periods of time [21,22]. Once the dye has been saturated, excitation of the sample and acquisition of images, using NIS-Elements Advanced research, are performed at various times for up to several days.

A single snapshot of the region at the contact line is shown in Fig. 2(a). The lighter region corresponds to the macroscopic part of the drop, whereas the dark region corresponds to the clean glass. A 3D representation of this snapshot is shown in Fig. 2(b), where the height of the film is proportionally related to light intensity. To investigate the time-dependent evolution of the diffusive precursor film, we followed the edge of the moving contact line as the drop spread and captured images over time. Figure 3, obtained by compiling the line profiles of the images taken at different times, reveals the development of the inflection point and the spreading of the film.

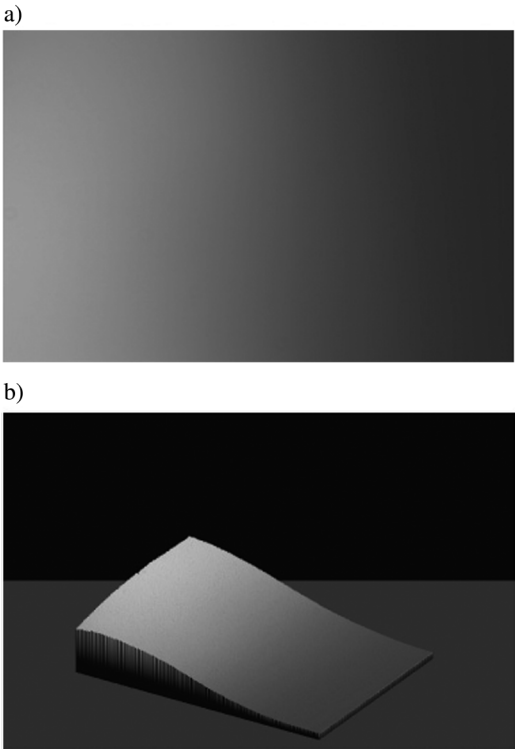

FIG. 2. (a) Image obtained from the contact line region of spreading silicone on glass substrate. (b) 3D representation of intensity and therefore film thickness as obtained by the image in (a).

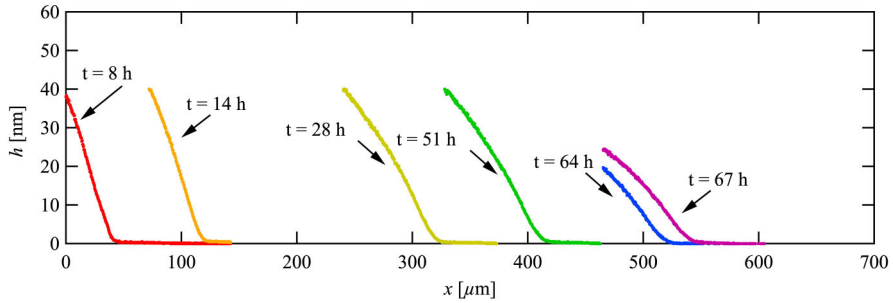

FIG. 3 (color online). Evolution of diffusive precursor film over time as a function of distance. Each line profile was captured by following the edge of the moving contact line as the drop continued to spread.

For a more quantitative analysis, we examined the profiles of drops for single instances of time. The experimental data exhibit the diffusive power law behavior and fits well to Eq. (2) for film thickness in the form $h = \beta(x - x_0)^n + h_0$. Figure 4 shows a profile at approximately 70 000 s after deposition. With the power n fixed as -2, the remaining fit parameters and their standard errors for this profile are as follows: $\beta = 2.98 \times 10^{-17} \pm 1.67 \times 10^{-18}$ m^3; $h_0 = 2.49 \times 10^{-9} \pm 9.12 \times 10^{-11}$ m; $x_0 = 4.25 \times 10^{-5} \pm 1.40 \times 10^{-6}$ m. The front factor β corresponds to an approximate Hamaker constant of $8 \times 10^{-20} \pm 4.41 \times 10^{-21}$ J, which agrees with values reported in the literature [23].

Figure 5 shows the length of the precursor film, which we measure from the inflection point to the point where thickness becomes zero, as a function of time. The inflection point is determined by taking the derivative of the experimental data with respect to the x direction (i.e., dh/dx) and finding the minimum. The fit in the form of $L = \alpha t^n + L_0$ is valid for times greater than 30 334 s after deposition, at which $L = 0$ signifies the emergence of the precursor film. With the power n fixed as 0.5, the fit parameters and their standard errors are as follows: $\alpha = 2.40 \times 10^{-7} \pm 1.01 \times 10^{-8}$ m/s$^{1/2}$; $L_0 = -4.18 \times 10^{-5} \pm 4.28 \times 10^{-6}$ m.

The inset of Fig. 5 emphasizes the power law fit for $L_p - L_0$ as a function of time. Our data match well with the theoretical power law as described by Eq. (1) and produce a similar Hamaker constant $1.05 \times 10^{-20} \pm 8.89 \times 10^{-22}$ J. This result reaffirms our experimental work as we independently arrive at values for Hamaker constant that are consistent with one another from two separate measurements—the length of precursor film and the shape of precursor film.

In summary, we have experimentally measured the time evolution of the diffusive precursor film for perfectly wetting van der Waals fluids using fluorescence microscopy. Our technique delivers sufficient range and resolution to address the challenge of capturing both the microscopic and macroscopic aspects of this phenomenon. We were able to observe the profile of a spreading drop from the spherical cap region to the inflection point from which

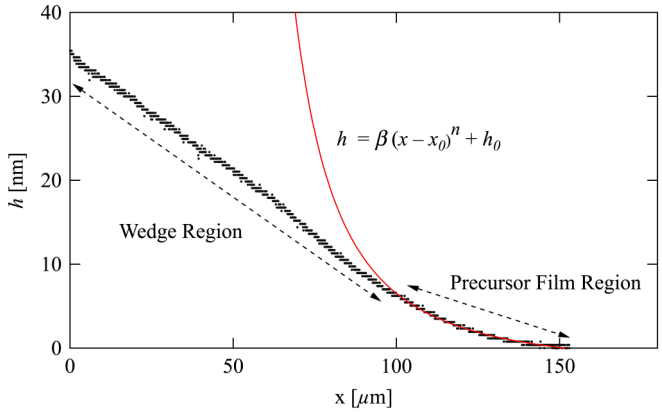

FIG. 4 (color online). Profile fit (line) of experimental data (dots) for the diffusive precursor film for a drop at $t = 69\,420$ s after deposition. With n fixed as -2, the remaining fit parameters and their standard errors are as follows: $\beta = 2.98 \times 10^{-17} \pm 1.67 \times 10^{-18}$ m^3, which corresponds to a Hamaker constant of $8 \times 10^{-20} \pm 4.41 \times 10^{-21}$ J; $h_0 = 2.49 \times 10^{-9} \pm 9.12 \times 10^{-11}$ m; $x_0 = 4.25 \times 10^{-5} \pm 1.40 \times 10^{-6}$ m.

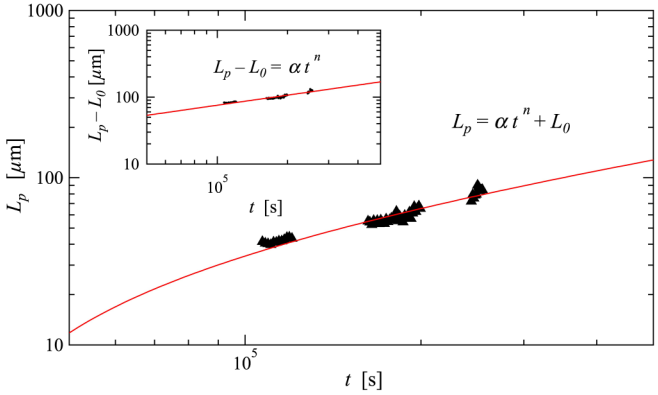

FIG. 5 (color online). Fit (line) of experimental data (triangles) for the length of the precursor film as a function of time. With n fixed as 0.5, the fit parameters and their standard errors are as follows: $\alpha = 2.40 \times 10^{-7} \pm 1.01 \times 10^{-8}$ m/s$^{1/2}$, which corresponds to a Hamaker constant of $1.05 \times 10^{-20} \pm 8.89 \times 10^{-22}$ J; $L_0 = -4.18 \times 10^{-5} \pm 4.28 \times 10^{-6}$ m. It should be noted that this equation is valid for times greater than 30 334 seconds after deposition, at which $L_p = 0$ (emergence of the diffusive precursor film). The inset of this figure shows the 0.5 power law for $L_p - L_0$ as a function of time.

the precursor film develops. The measurements presented here show good agreement with theoretical predictions and provide dynamic experimental data on microstructures in the vicinity of the moving contact line. These results offer valuable information for future numerical simulations of spreading, particularly in selecting appropriate parameters in the contact line region. Furthermore, our work demonstrates the potential of using fluorescence microscopy as a powerful technique for measuring thin film thicknesses.

We would like to thank Professor S. H. Davis, Professor G. M. Homsy, Professor H. A. Stone, and Professor L. Limat for helpful discussion. This research was supported by the National Science Foundation under Grant No. CBET-0730251 and the National Science Foundation GRFP, Grant No. DGE-0707424.

[1] S. F. Kistler, *Wettability* (Marcel Deker, New York, 1993), pp. 311–429.
[2] D. Bonn, J. Eggers, J. Indekeu, J. Meunier, and E. Rolley, Rev. Mod. Phys. **81**, 739 (2009).
[3] E. B. Dussan, Annu. Rev. Fluid Mech. **11**, 371 (1979).
[4] J. F. Joanny and P. G. de Gennes, J. Phys. (Paris) **47**, 121 (1986).
[5] L. H. Tanner, J. Phys. D **12**, 1473 (1979).
[6] O. Voinov, Fluid Dyn. **11**, 714 (1977).
[7] R. Homan, J. Colloid Interface Sci. **50**, 228 (1975).
[8] P. G. de Gennes, Rev. Mod. Phys. **57**, 827 (1985).
[9] H. P. Kavehpour, B. Ovryn, and G. H. McKinley, Phys. Rev. Lett. **91**, 196104 (2003).
[10] H. Hervet and P. G. de Gennes, C.R. Acad. Sci., Ser. II **299**, 499 (1984).
[11] W. B. Hardy, Philos. Mag. **38**, 49 (1919).
[12] D. Beaglehole, J. Phys. Chem. **93**, 893 (1989).
[13] F. Heslot, A. M. Cazabat, N. Fraysse, and P. Levinson, Adv. Colloid Interface Sci. **39**, 129 (1992).
[14] L. Leger, M. Erman, A. M. Guinet-Picard, D. Ausserre, and C. Strazielle, Phys. Rev. Lett. **60**, 2390 (1988).
[15] L. Leger, M. Erman, A. M. Guinetpicart, D. Ausserre, C. Strazielle, J. J. Benattar, F. Rieutord, J. Daillant, and L. Bosio, Rev. Phys. Appl. **23**, 1047 (1988).
[16] H. Xu, D. Shirvanyants, K. Beers, K. Matyjaszewski, M. Rubinstein, and S. S. Sheiko, Phys. Rev. Lett. **93**, 206103 (2004).
[17] T. Konisho and I. Ueno, Ann. N.Y. Acad. Sci. **1161**, 292 (2009).
[18] P. de Gennes, F. Brochard-Wyart, and D. Quere, *Capillarity and Wetting Phenomena: Drops, Bubbles, Pearls, Waves* (Springer, New York, 2004).
[19] P. Kavehpour, B. Ovryn, and G. H. McKinley, Colloids Surf. A **206**, 409 (2002).
[20] F. Rost, *Quantitative Uorescence Microscopy* (Cambridge University Press, Cambridge, U.K., 1991).
[21] G. Baillet, G. Giusti, and R. Guglielmetti, Bull. Chem. Soc. Jpn. **68**, 1220 (1995).
[22] J. Kim and M. Kim, Bull. Korean Chem. Soc. **26**, 966 (2005).
[23] A. Adamson and A. Gast, *Physical Chemistry of Surfaces* (Wiley, New York, 1997), 6th ed.